phase for three different IF frequencies and four different optical wavelengths (λ_1 = 1547.5nm, λ_2 = 1548.5nm, λ_3 = 1549.5nm, λ_4 = 1550.5nm) inside the CFG bandwidth are plotted, showing the expected linear response against detected frequency, with different slopes according to the CFG group delay at each wavelength. For each wavelength, the ripple around the ideally constant group delay (τ_1 = 934.6ps, τ_2 = 1762.0ps, τ_3 = 2595.8ps, τ_4 = 3441.3ps) against detected frequency has been calculated and the results show a worst case standard deviation of just ±0.9ps from 1 up to 20GHz.
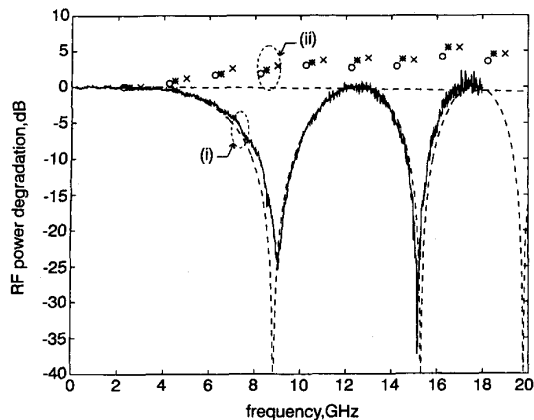

Fig. 2 *RF power degradation simulations and measurements of CFG-based delay line (conventional (m_o = 0.1, λ_0 = 1547.5nm) and PSH (m_{iF} = 0.1, m_{OL} = 0.6, λ_o = 1547.5nm) modulations*

(i) Conventional case
———— conventional case measurements
– – – – conventional case simulation
(ii) PSH
·········· PSH measurements
＊　　PSH measurements for ω_{IF} = 500MHz
○　　PSH measurements for ω_{IF} = 250MHz
✕　　PSH measurements for ω_{IF} = 1GHz
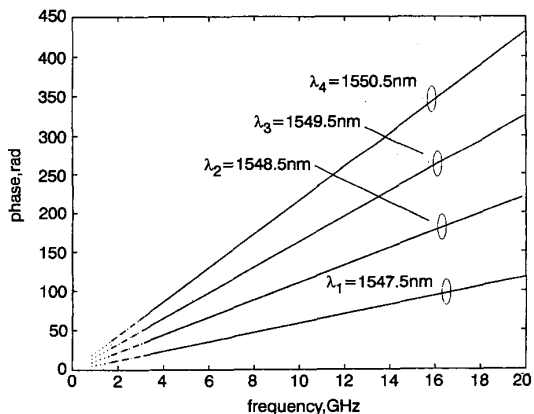– – – – PSH simulation (ω_{IF} = 1GHz)

Fig. 3 *Phase term at f_{RF} = $2f_{OL}$ + f_{IF} component of detected signal against detected frequency in CFG-based true time delay unit with PSH modulation (m_{iF} = 0.1, m_{OL} = 0.5) for four different optical wavelengths*

———— ω_{IF} = 1GHz
– – – – ω_{IF} = 250MHz
·········· ω_{IF} = 500MHz

Conclusion: A PSH modulation technique has been proposed for milimetre-wave time delay units based on CFG. With the PSH technique, the bandwidth requirements for the electro-optical modulation (IF and upconversion) are significantly smoothed. The first modulation stage is characterised by a low frequency modulation, while the upconversion requires a narrowband EOM. The amplitude and time delay theoretical results agree very well with the measurements on a time delay line with a 40cm long CFG at three different IF bandwidths (250MHz, 500MHz and 1GHz).

The detected signal amplitude shows a negligible dispersive attenuation up to 20GHz as opposed to conventional intensity modulating schemes. The estimated group delay for different optical wavelengths and intermediate frequencies shows a time ripple below ±0.9ps over a bandwidth of 1–20GHz. This result compares favourably with results obtained from SSB+C modulation techniques in which electrical compensation of the RF domain dispersion will lead to extra time delay ripple. The results shown in this Letter may also be extended to other dispersion-based delay lines, such as those with highly dispersive fibre instead of CFGs.

J.L. Corral and J. Marti (*ETSI Telecomunicacion, Universitat Politecnica de Valencia, Camino de Vera s/n, 46022 Valencia, Spain*)

E-mail: jlcorral@dcom.upv.es

P. Matthews and P. Biernacki (*Naval Research Laboratory, Code 5670, Washington, DC 20375, USA*)

References

1 ROMAN, J.E., FRANKEL, M.Y., MATTHEWS, P.J., and ESMAN, R.D.: 'Time steered array with a chirped grating beamformer', *Electron. Lett.*, 1997, 33, (8), pp. 652–653
2 CORRAL, J.L., MARTI, J., REOIDER, S., FUSTER, J.M., LAMING, R., and COLE, M.J.: 'Continuously variable true time delay optical feeder for phased array antenna employing chirped fibre gratings', *IEEE Trans. MTT/J. Lightwave Technol.*, Special Issue on Microwave Photonics, 1997, 45, (8), pp. 1531–1536
3 CORRAL, J.L., MARTI, J., FUSTER, J.M., and LAMING, R.I.: 'Dispersion-induced bandwidth limitation of variable true time delay lines based on linearly chirped fibre gratings', *Electron. Lett.*, 1998, 34, (2), pp. 209–211
4 FUSTER, J.M., MITI, J., and CORRAL, J.L.: 'Chromatic dispersion effects in electro-optical upconverted milimetre-wave fibre optic links', *Electron. Lett.*, 1997, 33, (23), pp. 1969–1970

Integrated optical LiNbO₃ distributed polarisation mode dispersion compensator in 20Gbit/s transmission system

R. Noé, D. Sandel, S. Hinz, M. Yoshida-Dierolf, V. Mirvoda, G. Feise, H. Herrmann, R. Ricken, W. Sohler, F. Wehrmann, C. Glingener, A. Schöpflin, A. Färbert and G. Fischer

Polarisation mode dispersion (PMD) in existing fibres impairs transmission at ≥ 10Gbit/s. A 43ps PMD compensator in X-cut, Y-propagation Ti:LiNbO₃ with cascaded TE-TM converters is presented and successful operation at 20Gbit/s demonstrated.

Introduction: Polarisation mode dispersion (PMD), caused by the anisotropy of existing optical fibres, is a serious obstacle in the development of highest-capacity, long-haul optical communication systems. PMD has been compensated for by selecting a principal state-of-polarisation (PSP) of the transmission line [1] or implementing an equaliser consisting of a small number of differential group delay (DGD) sections, separated by polarisation transformers [2 – 4]. We have recently presented a distributed fibre-based PMD equaliser [5]. Here PMD including higher orders is compensated for by functionally similar, birefringent LiNbO₃ devices. In contrast to previous approaches the integrated optics solution is compact, entirely non-mechanical, reliable, and features high speed.

Compensator structure: PMD can be represented by a sequence of three-dimensional vectors. Each has a length proportional to the DGD of a particular fibre section and differs in direction from its

predecessor according to the polarisation transformations in between them. A perfect PMD compensator mirrors the DGD profile of the transmission fibre and accurately follows its vector sequence in reverse direction back to the origin [5].

A PMD compensator with one DGD section will remove PMD only to first order, i.e. it will make the PMD vector sum equal to zero. However, residual higher-order effects will typically result in > 2dB (or infinite) penalty if the cancelled first-order DGD equals the bit duration T (or 1.4 T).

PMD compensators with one or few sections need to have variable DGD sections in order to avoid trapping in side maxima of a control signal which measures the eye opening. But a practical compensator with ≥ 2 sections cannot tolerate variable DGD sections: Consider a 52ps DGD change of one section. If DGD simply grows by this amount (10000 lightwave periods) at least one polarisation transformer following the variable DGD section has to turn 10000 times, which is incompatible with speed requirements. However two fixed 26ps DGD sections in the compensator can be made to either subtract or add their DGDs by turning a polarisation transformer just once.

Also, the transmission fibre does not require variable DGD sections in the compensator because its own DGD growth is negligible: Since a 52ps DGD change can occur by just one turn of a polarisation transformer in the middle of two 26ps sections of the transmission fibre a 52ps DGD growth, i.e. a 10000 times larger effect, is unlikely to occur.

The only viable possibility for near-perfect PMD equalisation lies therefore in compensators with fixed DGD sections. The section number should be so large that side maxima essentially coincide with the main maximum of the control signal.
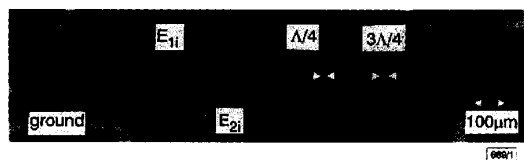

Fig. 1 *Photograph of mode converter electrode pair E_{1i}, E_{2i} (dark) in Ti:LiNbO$_3$ PMD compensator*

Device: TE-TM mode converters with coupling adjustable in both quadratures [6] have been chosen as polarisation transformers. Since they require X-cut, Y-propagation LiNbO$_3$ the natural birefringence (~0.26ps/mm) can be used for DGD cancellation at the same time. In Fig. 1 the interdigital electrodes covering the waveguide have periods equal to the optical beat length Λ, and subsequent interleaved combs are spaced by additional $\Lambda/4$ and $3\Lambda/4$ lengths. Operation is based on the electro-optic coefficient r_{51}. Depending on its phase each comb finger produces a small amount of mode coupling with ±45° linear or with right/left circular eigenmodes, respectively, in a waveguide section of length Λ. If there are many fingers the effects add and allow complete mode conversion with endlessly adjustable coupling phase [6].

A ~93mm long distributed PMD compensating device was fabricated with 73 cascaded mode converters of ~1.25mm length each, one of which is shown in Fig. 1. The efficiency was ~250V·mm for full conversion, and voltages of ±≤69V were applied. The insertion loss was 6.9dB, with a ±0.6dB variation depending on polarisation. Pigtailed chip and voltage sources form a compact unit. It was cascaded with a similar unit containing a somewhat shorter device. 246 voltages in total were used to control this PMD compensator with a combined DGD of 43ps. The calculated and measured conversion bandwidth of individual converters is ~3THz. If less optical bandwidth is needed some neighbouring electrodes can be driven together. This should considerably reduce the electronic effort and increase the control speed at the same time. Thermal tuning is possible with a rate of ~100GHz/K.

Experiment: The PMD compensator was tested (Fig. 2) in a 20Gbit/s transmission system [7] at a wavelength of 1565nm. Two polarisation-maintaining fibre sections with 20 and 10ps DGD, separated by motorised fibre optic waveplates rotating at different speeds, simulated the PMD of a fibre link (emulator). A controller maximised the power spectral densities of the received signal at 10

and at 5GHz [5]. The measured response time for full adaptation to a required compensation scenario was ~50ms. While this figure is satisfactory at present we expect that it can be improved significantly.

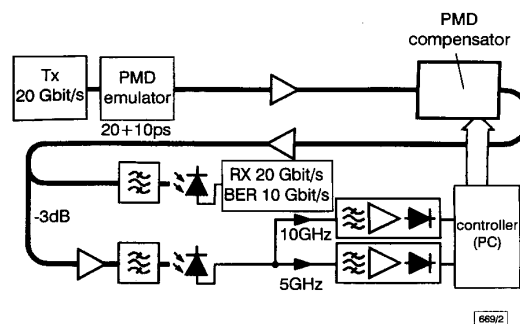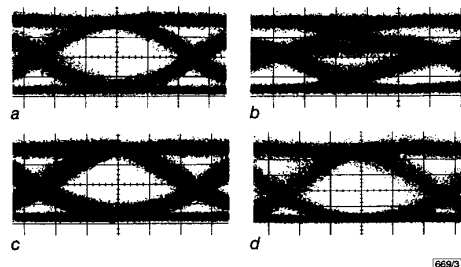**Fig. 2** *Experimental setup*

Fig. 3 *Eye diagrams*

a Back-to-back
b With emulator and idle compensator
c With emulator and working compensator
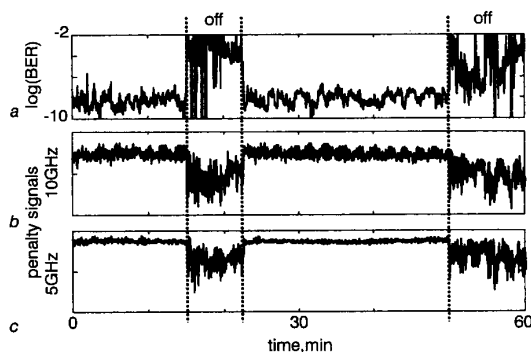*d* With compensator alone

Fig. 4 *Measured BER and power spectral densities at 10 and 5GHz while fibre optic waveplates rotate in PMD emulator*

a BER
b PSD at 10GHz
c PSD at 5GHz

The back-to-back eye diagram is shown in Fig. 3a. When the PMD emulator and idle compensator were in place, the eye (example: Fig. 3b) was often closed. With the working compensator the eye was well opened (Fig. 3c). When the PMD emulator was removed the compensator alone produced a very good eye pattern (Fig. 3d). Then the power was adjusted for BER ≈ 10⁻⁸, and the BER was recorded over time while the emulator with rotating fibre loops was in place. Stable operation over extended times was observed unless the compensator was switched off (Fig. 4). Owing to its many electrodes and large optical bandwidth we expect that it can also operate at higher bit rates.

Conclusions: A distributed 43ps PMD compensator with X-cut, Y-propagation Ti:LiNbO$_3$ devices has been realised. Accurate and fast equalisation of up to 30ps of differential group delay has been demonstrated in a 20Gbit/s transmission system.

R. Noé, D. Sandel, S. Hinz, M. Yoshida-Dierolf and V. Mirvoda
(Optical Communications and High-Frequency Engineering Department, University of Paderborn, Warburger Str. 100, 33098 Paderborn, Germany)

G. Feise, H. Herrmann, R. Ricken, W. Sohler and F. Wehrmann (Applied Physics Department, University of Paderborn, Warburger Str. 100, 33098 Paderborn, Germany)

C. Glingener, A. Schöpflin, A. Färbert and G. Fischer (Siemens AG, Information and Communication Networks, 81359 München, Germany)

E-mail: noe@uni-paderborn.de

References

1 ONO, T., YAMAZAKI, S., SHIMIZU, H., and EMURA, K.: 'Polarization control method for suppressing polarization mode dispersion influence in optical transmission systems', J. Lightwave Technol., 1994, LT-12, (5), pp. 891–898

2 TAKAHASHI, T., IMAI, T., and AIKI, M.: 'Automatic compensation technique for timewise fluctuating polarisation mode dispersion in in-line amplifier systems', Electron. Lett., 1994, 30, (4), pp. 348–349

3 HEISMANN, F., FISHMAN, D.A., and WILSON, D.L.: 'Automatic compensation of first-order polarization mode dispersion in a 10-Gbit/s transmission system'. ECOC '98, Madrid, Spain, Paper WdC11

4 SANDEL, D., YOSHIDA-DIEROLF, M., NOÉ, R., SCHÖPFLIN, A., GOTTWALD, E., and FISCHER, G.: 'Automatic polarisation mode dispersion compensation in 40Gbit/s optical transmission system', Electron. Lett., 1998, 34, (23), pp. 2258–2259

5 NOÉ, R., SANDEL, D., YOSHIDA-DIEROLF, M., HINZ, S., GLINGENER, C., SCHEERER, C., SCHÖPFLIN, A., and FISCHER, G.: 'Polarisation mode dispersion compensation at 20Gbit/s with fibre-based distribution equaliser', Electron. Lett., 1998, 34, (25), pp. 2421–2422

6 HEISMANN, F., and ULRICH, R.: 'Integrated-optical single-sideband modulator and phase shifter', IEEE J. Quantum Electron., 1982, 18, (4), pp. 767–771

7 BOGNER, W., FISCHER, U., GOTTWALD, E., and MÜLLNER, E.: '20Gbit/s TDM nonrepeatered transmission over 198km DSF using Si-bipolar IC for demultiplexing and clock recovery'. ECOC '96, Oslo, Norway, Vol. 2, pp. 203–206

Observation of light propagation in photonic crystal optical waveguides with bends

T. Baba, N. Fukaya and J. Yonekura

Light propagation is investigated in two-dimensional photonic crystal waveguides with bends, which were composed of closely-packed holes formed in a GaInAsP thin film. Wavelength and polarisation dependence on propagation characteristics were observed in the wavelength range 1.47–1.60μm.

Photonic crystals can be used as omni-directional mirrors with high reflectivity due to the photonic bandgap (PBG). One of the suggested potential applications is for a waveguide with strong optical confinement, in which photonic crystals are used as claddings. Low loss propagation through waveguides with sharp bends, branches etc., has been theoretically estimated [1, 2], and some experimental demonstrations have been presented involving the use of a large crystal for millimetre waves [3]. However, experiments are much more difficult for lightwaves. Light propagation in straight waveguides has been recently investigated [4]. Still, the effect of photonic crystal claddings was not made clear, since the waveguide was as short as several micrometres. In this Letter, we report the first observation of light locus in such waveguides with bends.

In this study, a GaInAsP film epitaxially grown on InP substrate was used as the waveguide material. The thickness and bandgap wavelength were 0.35 and 1.38μm, respectively. It was bonded using a thin epoxy onto a host substrate, the surface of which was covered with a 3μm thick SiO_2 film. The first InP substrate was then removed by selective wet etching. Thus, the GaInAsP film acts as a slab waveguide with upper air and lower SiO_2 claddings. Before the bonding process, a two-dimensional (2D)

photonic crystal was formed in the GaInAsP film by electron beam lithography and dry etching. It was composed of closely packed holes. The designed diameter and hole pitch were 0.5 and 0.6μm, respectively. According to 2D photonic band calculations, full PBG is realisable in the wavelength range $\lambda = 1.5–1.6\mu m$ when the refractive index of the semiconductor is 3.38 [5]. A channel waveguide was composed of a single line of defects of the crystal, i.e. a GaInAsP corrugated stripe with 0.7μm minimum width. The photonic crystal pattern includes straight waveguides 25μm in length with 60° or 120° bend. Fig. 1 shows the crystal before the bonding process. Holes just beside the waveguides became 20–30% smaller than the designed hole due to nonuniform exposure during the lithography process, while other holes were almost the same size as the designed one. After the bonding process, however, the waveguide width was expanded to 2.4μm, since the dry etching did not pierce the smaller holes.
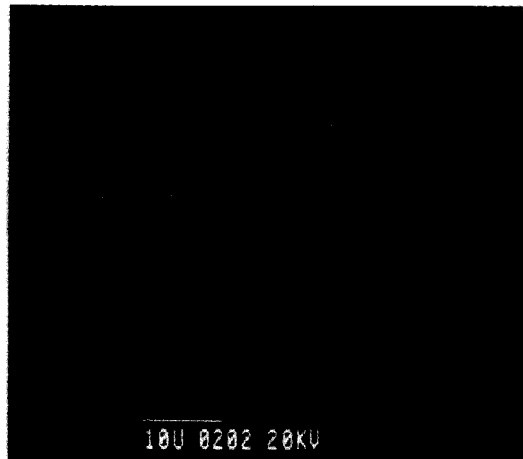

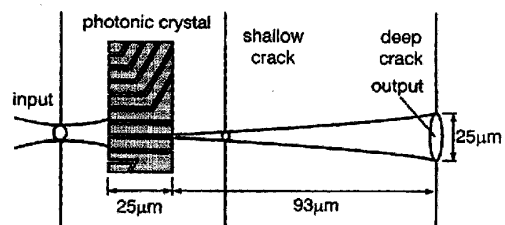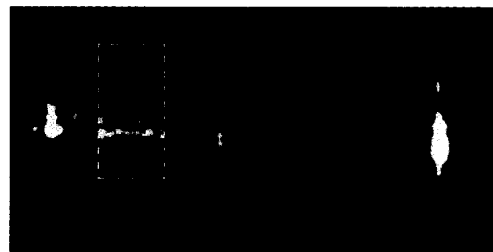Fig. 1 Top view of formed photonic crystal with defect waveguides

Fig. 2 Near field image and schematic diagram of waveguide surface

– – – – position of photonic crystal

In the measurement, a tunable laser with $\lambda = 1.47–1.60\mu m$ was used as a light source. The light was focused on a cleaved facet of the sample. The light locus was observed from the top of the surface using an infrared TV camera. For the film without the photonic crystal and unexpected defects, the light locus was not observed due to the small surface scattering of light. Light propagation in the slab waveguide was confirmed over the above wavelength range from the scattered light at some cracks of the film, which might be caused by the residual tension in the epoxy. We considered that it was a guided mode in the GaInAsP, not a cladding mode in the SiO_2, since the calculated propagation loss of the cladding mode was as large as 43–45dB/mm for arbitrary polarisation. For a channel waveguide, we confirmed the light propaga-